

HYBRID SLIDING-ROCKING POST-TENSIONED SEGMENTAL BRIDGES: LARGE-SCALE QUASI-STATIC AND SHAKE TABLE TESTING

P. Sideris, A. J. Aref & A. Filiatrault

University at Buffalo – The State University of New York, U.S.A.



SUMMARY:

In this paper, the novel concept of hybrid sliding-rocking (HSR) post-tensioned segmental members for seismic applications in bridges is presented. Fundamental components of these members are the HSR segmental joints coupled with internal unbonded post-tensioning (PT). The HSR joints can potentially exhibit sliding and/or rocking to mitigate the applied seismic loading. The joint response is controlled by the geometry of the PT system, which can follow linear or nonlinear layouts along the member length. Two distinct types of HSR members are considered; those with slip-critical joints and linear PT geometry, intended for bridge substructures, and those with rocking-critical joints and nonlinear PT geometry, intended for bridge superstructures. A two stage experimental study validated the seismic performance of the proposed HSR system. The first stage included shake table testing on a large-scale bridge specimen, while the second stage included quasi-static cyclic testing of the specimen's substructure.

Keywords: segmental construction; seismic testing; bridges; post-tensioning; sliding-rocking

1. INTRODUCTION

Superstructures and substructures of precast concrete segmental bridges consist of a number of segments post-tensioned together by several, typically bonded, tendons. Shear keys and epoxy adhesives are used at the segmental joints to provide resistance against shear (sliding) and tension (opening/separation). This approach emulates the cast-in-place concrete systems and is intended to make segmental bridges respond as if they were monolithic.

In the past three decades, the number of precast concrete segmental bridges has increased substantially both in the United States and around the world, mainly due to the advantages that segmental construction offers compared to the traditional cast-in-place techniques. These advantages primarily relate to: (i) higher construction quality, since the segments are constructed in precast plants under high quality control, and (ii) rapid construction, considering that as soon as the segments are delivered to the construction site, only assembly and preparation of the joint connections are required. The significant reduction of the on-site construction time gave this method, over the years, the name "Accelerated Bridge Construction (ABC)".

Despite the evident advantages that precast segmental bridge systems offer, their application has been limited only to low seismicity areas, primarily due to the fact that their seismic performance is largely unknown. In this paper, a novel segmental bridge system, intended for moderate and high seismicity areas, is proposed and its seismic performance is validated experimentally. The proposed system incorporates hybrid sliding-rocking (HSR) post-tensioned segmental members and is applicable to both superstructures and substructures. The HSR members combine two fundamental components: (i) HSR

segmental joints, and (ii) Internal unbonded post-tensioning (PT) of linear or nonlinear geometry along the member length. The HSR joints are simple friction-type connections defined by direct plane surface-to-surface contact between adjacent segments without shear keys. The HSR joints utilize relative segment-to-segment sliding (joint sliding) and gap opening (joint rocking) to mitigate the applied seismic loading. Joint sliding provides energy dissipation with negligible damage, which is an appealing attribute for seismic applications, as well as moderate self-centering. On the other hand, joint rocking provides lower energy dissipation, but high self-centering that deteriorates at larger rocking rotations due to concrete crushing at the joint edges. The response of HSR joints is directly influenced by the geometric layout of the PT tendons along the member's length. Thus, linear or nonlinear PT geometry can be used to achieve target joint response properties.

The concept of HSR members is validated by a two-stage experimental study. The first stage includes shake table testing on a large-scale single-span bridge specimen, while the second stages includes quasi-static cyclic testing of the segmental piers. The experimental program was conducted in the Structural Engineering and Earthquake Simulation Laboratory (SEESL) of the University at Buffalo (UB), U.S.A.

Note that the objective of this paper is to provide only a brief presentation of the proposed HSR members. Further information on the proposed system may be found in Sideris et al. (2012), while a complete presentation of the HSR concepts and detailed description of their experimental and numerical validation is provided in Sideris (2012).

2. SYSTEM DESCRIPTION

2.1. Hybrid Sliding-Rocking Segmental Joints with Unbonded Post-tensioning

The response of HSR joints coupled with internal unbonded post-tensioning is discussed with respect to the member shown in Figure 1 (a). The member consists of two segments post-tensioned with two straight internal unbonded tendons and is fixed at its base; hence, it has a single segmental joint at the mid-height. At the segment ends adjacent to that joint, the ducts accommodating the PT system have been substituted by duct adaptors, which are pieces of tubing of larger diameter than that of the ducts. No epoxy adhesives or shear keys have been used at the joint. Application of post-tensioning is followed by application of a constant compressive axial force P_2 and, then, a monotonically increasing lateral force P_1 . Based on the forces applied to the joint (i.e. axial, shear and moment), the geometric properties of the joint, and the frictional properties at the joint interface, joint response may initiate either with sliding (slip-critical joint) or rocking (rocking-critical joint).

In the case of a slip-critical joint, sliding continues until either joint rocking becomes critical or the joint sliding (amplitude) capacity is reached (i.e., sliding limit at which the tendons come in contact with both the top and bottom duct adaptors), as shown in Figure 1 (b.2). In the latter case, further increase of P_1 leads to joint rocking as depicted in Figure 1 (b.3). As demonstrated in Figure 1 (b.2), the diameter of the duct adaptors controls the joint sliding (amplitude) capacity. Resistance against joint sliding is provided by the friction force at the joint interface and the tendon bearing forces (dowel effect) on the ducts and duct adaptors (see Figure 1 (b.2)). However, re-centering is only provided by the tendon bearing forces. Tendon bearing forces are activated when the tendon come in contact with the duct at the location where duct and duct adaptor meet. At this location, the sliding displacement equals the difference in diameter between the duct and the tendon. The tendon bearing forces are maximized when the joint sliding capacity is reached (i.e., when the tendon comes in contact with the top and bottom duct adaptors at the location of the joint, as shown in Figure 1 (b.2)). The variation of the tendon bearing forces between these two extreme values is controlled by the length of the duct adaptor, as illustrated in Figure 1 (b.2). Hence, for shorter duct adaptors, higher bearing forces are generated at smaller joint sliding displacements.

If the joint is rocking-critical, the response will initiate with joint rocking, in the form of partial gap opening at the joint interface. As P_1 increases, joint rocking increases, while sliding may become critical at a reduced contact area, especially if the coefficient of friction varies with the contact pressure. Consequently, transition to joint sliding or co-existence of sliding and rocking is possible.

During joint rocking, resistance and re-centering is provided by the PT system as well as the load P_2 (as long as it remains compressive). The fact that the major re-centering forces (i.e., PT forces) against joint rocking are active before joint opening and their magnitude increases as joint opening increases provides the rocking mode with considerable self-centering capabilities. These self-centering capabilities deteriorate at larger rocking rotations due to the concrete crushing and potential tendon yielding. Concrete damage and tendon yielding are the only energy dissipative mechanisms of this mode which typically exhibits low energy dissipation characteristics. In contrast, joint sliding offers significant energy dissipation capabilities (due to friction) with minor or negligible damage, since sliding only causes wearing of the joint interface, but no significant structural damage. To achieve target frictional properties, treatment of this interface should be considered through application of epoxy materials or other means. The moderate self-centering capabilities of the slide mode are attributed to two facts: (i) the frictional resistance is hysteretic with respect to sliding; hence, not self-centering, and (ii) the bearing tendon forces remain inactive before a sliding threshold (initiation of contact between tendon and ducts) is reached; hence they cannot overcome the frictional resistance at lower sliding amplitudes. The amount of residual joint sliding is controlled by the joint frictional properties and the variation of the tendon bearing forces with the sliding displacement.

Under base excitation, P_1 could be assumed to represent the seismic force generated by a mass supported on top of the member in Figure 1 (a), while P_2 could represent the corresponding gravity load and vertical excitation effects. In this case, both joint sliding and rocking would provide control of the applied seismic loading by: (i) limiting the joint strength, which would directly control the amplitude of the applied forces, and (ii) reducing the joint stiffness, which would lead to lengthening of the system natural periods. The characteristics of the earthquake excitation would also affect the amount of residual joint sliding.

As an alternative to the linear PT geometry of Figure 1 (a), the nonlinear PT geometry of Figure 1 (c.1), can be used. In this case, the tendons will be in bearing contact with the ducts immediately after application of post-tensioning, resulting in activation of significant resisting forces, even for minor joint sliding (see Figure 1 (c.2)). Thus, nonlinear PT geometry can be used as a means of restraining joint sliding.

2.2. Hybrid Sliding-Rocking Post-tensioned Segmental Members

Based on the type of HSR joints (slip- or rocking-critical) that a member incorporates, different member response properties are achieved. In this study, two distinct types of HSR members are considered: (i) HSR members with slip-critical joints and linear PT geometry (abbreviated as HSR-SC members), and (ii) HSR members with rocking-critical joints and nonlinear PT geometry (abbreviated as HSR-RC members). The seismic response properties of these member types are dictated by the response properties of the corresponding dominant joint response modes.

A major response characteristic of HSR-SC members over conventional and rocking-only segmental members is their inherent capability of providing energy dissipation with low or negligible damage through joint sliding. For seismic applications, this is an attractive property that can eliminate the need for supplemental energy dissipation, typically provided by external devices in rocking-only members. Furthermore, potential residual joint sliding is not associated with structural damage and can be restored by various means (Sideris 2012). These response properties make the HSR-SC members particularly appealing for substructure systems. On the contrary, HSR-RC members are more suitable for

superstructures, which typically incorporate nonlinear PT geometry and they are more sensitive to residual deformations.

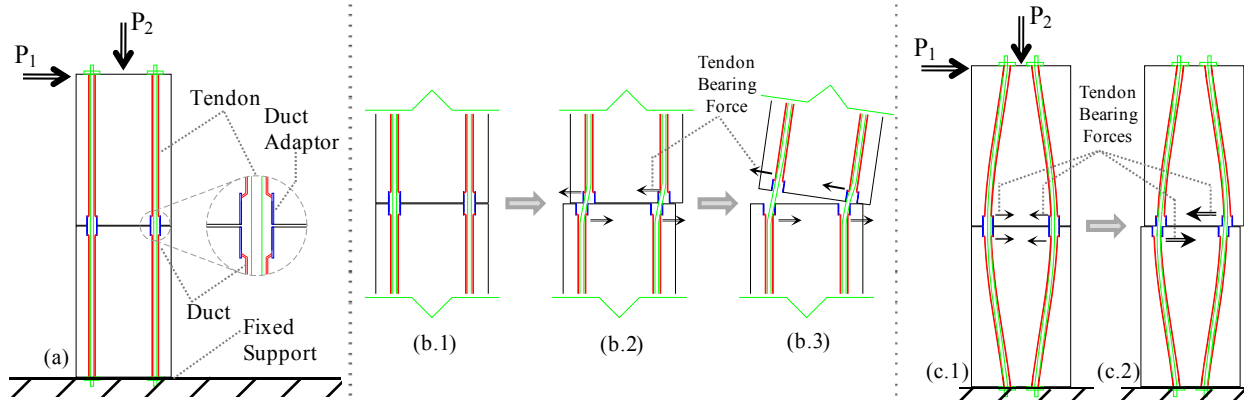


Figure 1. (a) Benchmark configuration (b) Slip-critical HSR joint: (b.1) Undeformed configuration, (b.2) Sliding capacity reached, and (b.3) Rocking response, after sliding capacity has been reached, and (c) Benchmark configuration with nonlinear PT geometry: (c.1) Undeformed configuration, and (c.2) Response against sliding

A fundamental response property of HSR-SC members (e.g., HSR-SC pier columns) is the *migration* of joint sliding from a single joint to several adjacent joints as the displacement demand increases. Joint sliding migration is caused by the tendon bearing forces, which significantly increase the shear sliding strength of a given joint at large sliding amplitudes (towards the sliding capacity of the joint, see Figure 1 (b.2)). As a result of this increase in the joint shear strength, sliding propagates at the neighboring joints, which, at the time, have lower shear sliding strength.

3. EXPERIMENTAL VALIDATION

The seismic performance of the proposed HSR members is validated through a two-stage experimental study, including shake table and quasi-static cyclic testing on a large-scale single-span bridge specimen.

3.1. Shake Table Testing of a Large-scale Bridge Specimen

3.1.1. Specimen Description

The experimental specimen was a large-scale (~1:2.39) single-span single-cell box girder precast concrete segmental bridge with both of its supports overhanging at equal lengths of 25% of the length of the span. The test specimen represented the mid-span of the prototype five-span single-cell box girder concrete bridge considered by Megally et al. (2002). The length of the specimen's superstructure was 61.9 ft (18.9 m) with a pier-to-pier distance of 41.9 ft (12.9 m), while the height of each pier (including the cap beam, but not the foundation block and the superstructure) reached 11.9 ft (3.6 m). The specimen is shown mounted on the dual shake tables of SEESL at UB in the photograph of Figure 2 (a).

The bridge specimen consisted of a HSR-RC superstructure and two single-column HSR-SC piers. The superstructure consisted of eight hollow segments of trapezoidal cross-section which were post-tensioned together by 12 internal unbonded tendons; 10 harped-shaped and two straight (located at the top flange). On the other hand, each pier consisted of five segments of hollow square cross-section that were post-tensioned together by eight straight internal unbonded tendons. The superstructure cross-section is shown in Figure 2 (b), while the pier segment is illustrated in plan and elevation view in Figure 2 (c) and (d), respectively. The PT system of the superstructure is shown in elevation and plan view in Figure 3 (a) and (b), respectively, while the PT system of the substructure is illustrated in Figure 3 (c). A cap beam of

trapezoidal solid shape was placed on top of each pier to facilitate support of the superstructure, whereas a foundation block was attached at the bottom of each pier to allow mounting of each pier on one of the two relocatable shake tables of SEESL (see Figure 2 (a)). The foundation block, the cap beam and the five pier segments shared the same PT tendons, as shown in Figure 3 (c). The superstructure was simply supported on the cap beams, while no bearings or pads were considered at the superstructure-to-cap beam interfaces.

Tendons of 0.5” (1.27 cm) and 0.6” (1.52 cm) diameter were used at the superstructure and substructure, respectively, and were accommodated by ducts of the same interior diameter of 0.9” (2.29 cm). To further restrain potential joint sliding, no duct adaptors were used in the superstructure. On the contrary, duct adaptors of interior diameter of 1.375” (3.49 cm) and length of 1.5” (3.81 cm) were used at both ends of all pier segments, as shown in Figure 2 (d). At full engagement of the tendons with the duct adaptors (or ducts) at both sides of a joint, the resulting nominal joint sliding capacity was: (i) 0.4” (= 0.9” - 0.5”) or 1.02 cm (= 2.29 cm - 1.27 cm) at the superstructure, and (ii) 0.775” (= 1.375” - 0.6”) or 1.97 cm (= 3.49 cm - 1.52 cm) at the substructure. A thin layer of silicone material was applied to all pier joints to provide uniform frictional properties over the joint interface and reduce the concrete-to-concrete coefficient of friction to the target range. The achieved coefficient of friction was in the range of 0.07 to 0.10. Silicone material was not applied to the superstructure joints, where larger coefficients of friction were desired to prevent sliding. To minimize stress concentration at the superstructure joints, all segments were constructed with the “match-cast” method, according to which each segment was cast while in contact with its adjacent one. Stress concentration at the pier joints was alleviated by interface treatment combined with application of the silicone material.

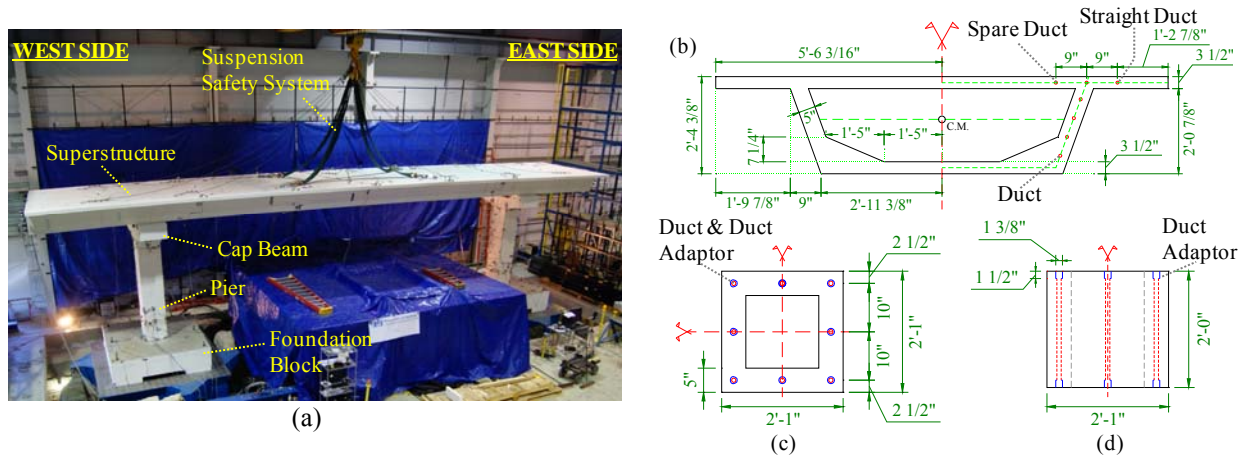


Figure 2. Precast concrete segmental bridge specimen (1’ = 12”, 1” = 2.54 cm): (a) Mounted on the two relocatable shake tables in SEESL at University at Buffalo, (b) Superstructure cross-section, (c) Pier segment – Cross-section, and (d) Pier segment – Elevation view

The design of the bridge specimen was conducted according to the AASHTO LRFD Bridge Design Specifications (2007) and partially assisted by the PCI Bridge Design Manual (2003). The seismic hazard considered was associated with a site in the Western United States, while the vertical hazard was taken as 2/3 of the horizontal hazard, which is a typical assumption in practice, as stated in the ATC/MCEER Joint Venture (2003). To further challenge the ductility capacity, energy dissipation and self-centering capabilities of the HSR members, response modification factors, R, larger than those recommended by AASHTO LRFD Bridge Design Specifications (2007) were used for the design of both the superstructure (R=2.5 instead of 1) and the substructure (R=2.5×1.5=3.75 instead of 1.5).

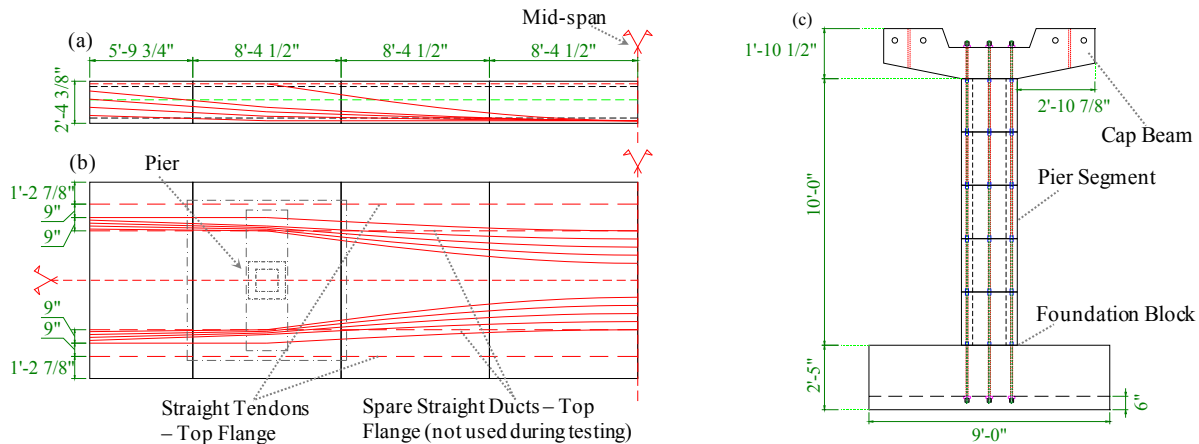


Figure 3. Post-tensioning system (1' = 12", 1" = 2.54 cm): (a) Superstructure – Elevation view, (b) Superstructure – Plan view, and (c) Pier – Elevation view

3.1.2. Shake Table Testing

The test specimen was subjected to a large number of shake table tests (nearly 150) with far-field and near-fault ground motions scaled to several seismic hazard levels, including the Design Earthquake (DE – probability of exceedance (PoE): 10% in 50 years) given by the AASHTO LRFD Bridge Design Specifications (2007) and the Maximum Considered Earthquake (MCE – PoE: 2% in 50 years) defined as 3/2 of the DE hazard as recommended by ASCE/SEI 7-05 (2006). Results from a single test are employed to demonstrate key response characteristics of the proposed HSR members. In this test, the specimen was subjected to the lateral and vertical component of a motion (ID No. 5 per FEMA P695 2009 – Delta station, owned by UNAM / UCSD) recorded during the 1979 Imperial Valley earthquake. The lateral component of this motion was scaled to a seismic hazard that exceeded the MCE event, whereas the vertical component was scaled to approximately 2.4 times the hazard of the lateral component. The 5%-damped acceleration response spectra of the horizontal and vertical components of the motions recorded at the foundation blocks are compared with the corresponding DE and MCE spectra in Figure 4 (a) and (b), respectively. At the fundamental periods of the system (approximately 0.44 sec and 0.14 sec in the lateral and vertical direction, respectively, before that test), the MCE hazard was exceeded by approximately 40% and 70% in the lateral and vertical direction, respectively.

The hysteretic response of both HSR-SC piers (i.e., base shear force versus lateral displacement on top) is presented in Figure 4 (c). As shown, both piers provide energy dissipation and self-centering capabilities. The energy dissipation is more pronounced at smaller displacement amplitudes, as indicated by the “fatter” hysteresis loop, particularly for the east pier. In contrast, the self-centering capabilities become more dominant at larger displacement amplitudes. Such response characteristics result from the fact that HSR-SC members initially (i.e., at smaller displacements) respond with joint sliding at several joints, while as the displacement demand increases, joint rocking is exhibited, primarily at the bottom joints. As a result of the initial joint sliding, HSR-SC members exhibit stronger energy dissipation capabilities at smaller displacements, but moderate self-centering capacity. In contrast, the subsequent joint rocking response reduces the energy dissipation capacity of the HSR-SC members, but considerably enhances their self-centering capabilities. The joint sliding hysteresis (i.e., joint shear versus joint sliding) and joint rocking hysteresis (i.e., joint moment versus joint rocking) at the two lower joints of both piers are presented in Figure 5 (a) and (b), respectively. The joint identification, JE0 and JE1, represents the bottom joint and the second joint from the bottom of the east pier, respectively. Similarly, the nomenclature, JW0 and JW1, refers to the corresponding joints of the west pier. Substantial sliding is observed at the joints JE1 and JW1, while sliding is small at the two bottom joints, JE0 and JW0. In contrast, considerable rocking is observed at the two bottom joints, JE0 and JW0, whereas rocking is negligible at the joint JE1

and JW1. These hysteresis plots also demonstrate the energy dissipation characteristics of joint sliding as well as the self-centering properties of joint rocking.

The response of the HSR-RC superstructure in the vertical direction was dominated by the first node, which resulted in considerable joint rocking at mid-span. According to the rocking hysteresis at mid-span, shown in Figure 5 (c), the rocking mode exhibited high self-centering capacity and low energy dissipation properties. As a result, the residual vertical displacement of the superstructure was negligible.

The capacity of both the HSR-SC and HSR-RC to control the applied seismic loading results from their controlled stiffness and strength properties as demonstrated by the corresponding measured hysteresis loops.

Inspection of the bridge specimen at the end of this test revealed that the HSR-SC piers sustained only minor damage, albeit the input excitation significantly exceeded the MCE hazard level and the piers were designed for $R=3.75$. Larger damage was prevented by the considerable joint sliding as demonstrated by the measured data. The observed damage was in the form of spalling of the concrete reinforcement cover in the vicinity of the second from the bottom joint as a result of sliding, and limited concrete crushing at the bottom joint due to the high moment demand. For the HSR-RC superstructure, the damage was insignificant, while negligible joint sliding was also observed at all joints—even those close to the supports, which were subjected to the largest shear forces. This response is attributed to the combined effect of nonlinear PT geometry, dry friction, and small allowable joint sliding capacity.

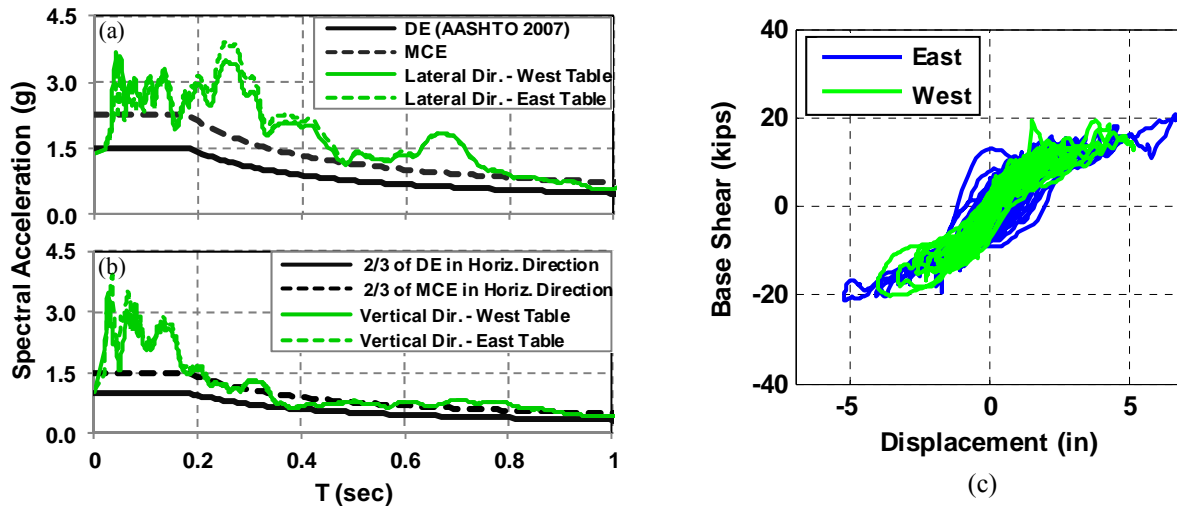


Figure 4. (a) Response spectra ($\xi=5\%$) of lateral motions recorded at the foundation blocks versus DE (AASHTO LRFD Bridge Design Specifications 2007) and MCE ($1.5\times$ DE) spectra, (b) Response spectra ($\xi=5\%$) of the vertical motions recorded at the foundation blocks versus DE and MCE spectra (defined as 2/3 of corresponding horizontal hazard), and (c) Base shear versus top displacement for both piers

3.2. Quasi-static Cyclic Testing of Bridge Piers

3.2.1. Specimen Description and Test Execution

Shake table testing of the bridge specimen was followed by quasi-static testing of the HSR-SC piers. The objective of this experimental stage was to investigate the response of the HSR-SC piers at displacement demands, much larger than those imposed during shake table testing. The effect of dead and live loads was simulated by two vertical “gravity” PT tendons (of 21 kips – 93.5 kN each) attached to the two sides of the cap beam, as shown in Figure 6 (a). Cyclic loading of increasing amplitude was applied in displacement control by the two actuators shown in Figure 6 (a). The loading rate was in the range of 0.01

– 0.05 in/sec (0.025 – 0.13 cm/sec). Two loading cycles were considered for each prescribed displacement amplitude. All force signals were corrected for the weight of the actuators and the lateral contribution of the gravity tendons. Both piers exhibited similar qualitative and quantitative response. Results from testing of one pier are presented below.

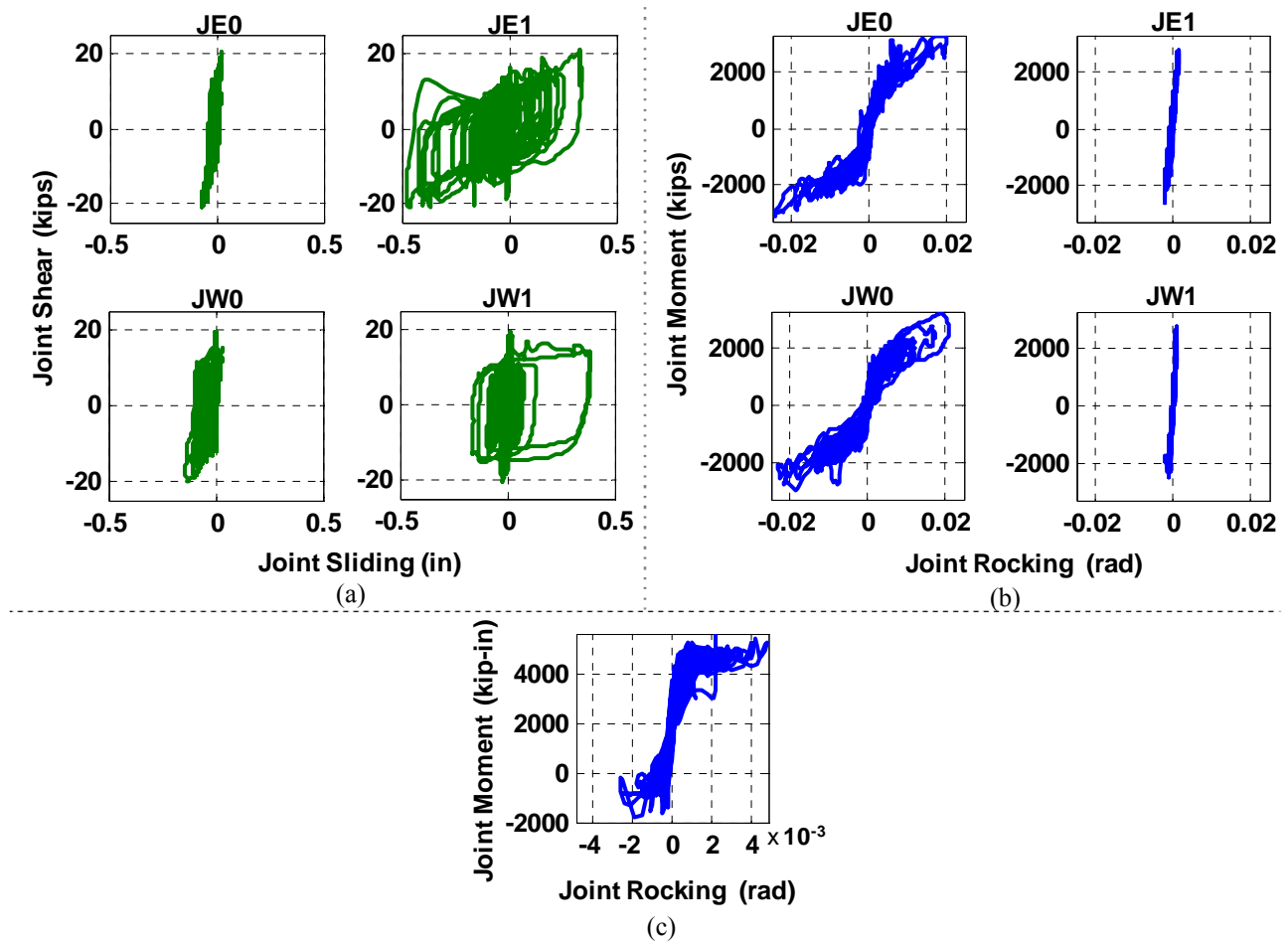


Figure 5. HSR joint response (1 kip= 4.45 kN, 1 in = 2.54 cm): (a) Joint shear force vs. joint sliding, and (b) Joint moment vs. joint rocking

According to the measured hysteresis shown in Figure 6 (b), the HSR-SC pier provides large ductility capacity reaching an ultimate displacement drift ratio of approximately 14.9%. The deformed shape at the ultimate drift ratio is shown in Figure 6 (b). All joints exhibited substantial sliding, whereas large rocking was only observed at the bottom joint. The joint sliding and rocking hysteresis at the bottom joint (J0) and second from the bottom joint (J1) are presented in Figure 7 (a) and (b), respectively. The rocking and sliding response for the rest of the joints was similar to that of joint J1. At smaller drift ratios (< 5%), joint sliding controlled the response and the energy dissipation capacity of the pier was larger. This is demonstrated by both the sliding energy ratio (SER, i.e., the ratio of the energy dissipated due to joint sliding over the total dissipated energy) and the equivalent viscous damping ratio (estimated as in Chopra (2001)) shown in the top and bottom plots, respectively, of Figure 7 (c). At smaller displacements, joint sliding dissipated over 75% of the total dissipated energy, while the equivalent damping ratio exceeded 30%. In contrast, at larger drift ratios (> 10%), SER reduced to 35 – 40%, while the damping ratio reduced to 16 – 17%. Furthermore, at larger drift ratios (> 10%), self-centering increased (see Figure 6 (b)), since the response was controlled by the joint rocking at the bottom.

Post-test inspection of the specimen revealed concrete crushing at the bottom joint (J0) due to the large moment demands. No structural damage, other than concrete spalling of the reinforcement cover in the vicinity of all joints, was observed as a result of joint sliding. The negligible damage associated with joint sliding is also demonstrated by the stable joint sliding hysteresis measured at all joints (e.g., bottom plot of Figure 7 (a)).

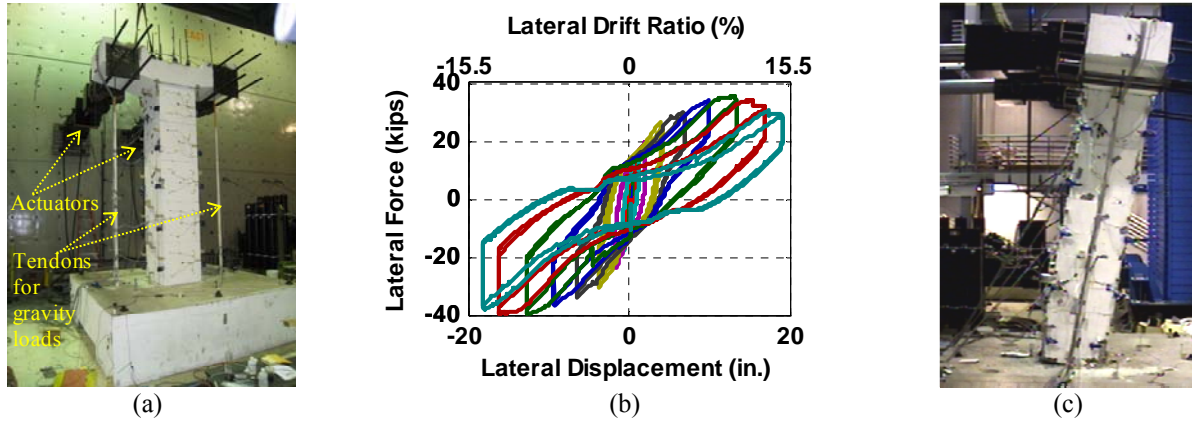


Figure 6. (a) HSR-SC pier joint, before testing, (b) Pier hysteresis (1 kip= 4.45 kN, 1 in = 2.54 cm), and (c) HSR-SC pier at ultimate drift ratio (~14.9%)

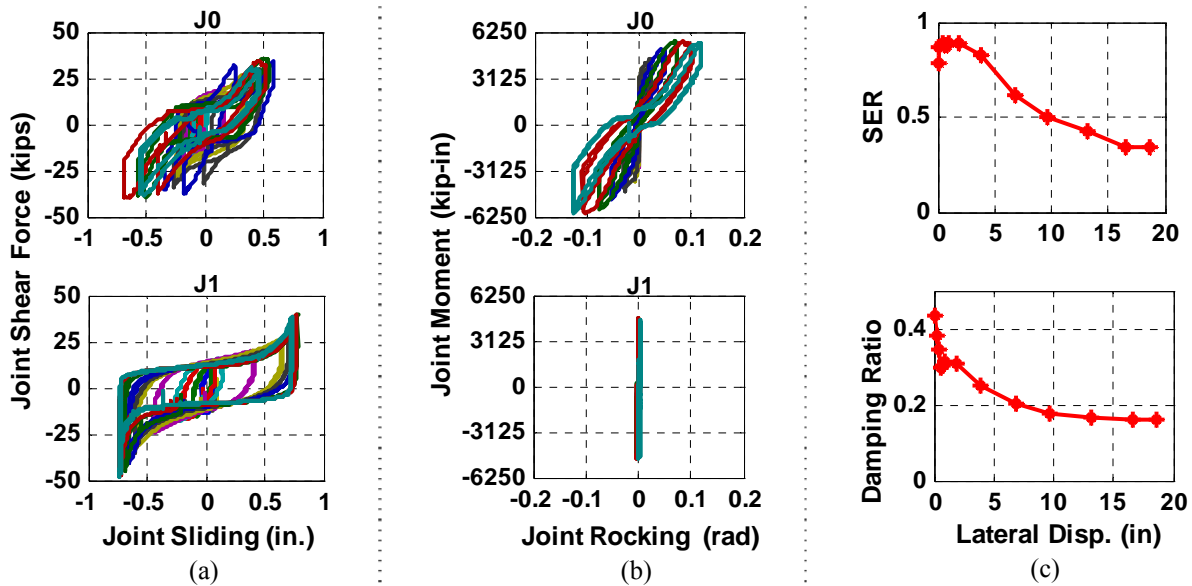


Figure 7. (a) Joint sliding hysteresis at the two lower joints, (b) Joint rocking hysteresis at the two lower joints, and (c) Sliding energy ratio (SER) and equivalent damping ratio (1 kip= 4.45 kN, 1 in = 2.54 cm)

4. CONCLUSIONS

In this paper, the concept of hybrid sliding-rocking (HSR) post-tensioned segmental members for bridge systems in seismic regions was presented and validated experimentally. The HSR members consist of HSR joint coupled with internal unbonded post-tensioning (PT) of linear on nonlinear geometric layout along the member length. Two distinct HSR member types were studied; those with slip-critical joints and linear PT geometry (abbreviated as HSR-SC members) and those with rocking-critical joints and non-linear PT geometry (abbreviated as HSR-RC members).

The proposed system was validated by a two-stage experimental study for a large-scale single-span bridge specimen with HSR-RC superstructure and two single-column HSR-SC piers. The first stage included an extensive series of shake table tests (nearly 150) on the bridge specimen, while the second stage included quasi-static cyclic testing of the piers. The HSR-SC piers exhibited substantial energy dissipation capacity, large ductility, moderate self-centering. Moderate damage was also observed in the form of concrete crushing at the bottom and spalling in the vicinity of the HSR joints, while joint sliding was found to be a low-damage response mode. On the other hand, the HSR-RC superstructure exhibited low energy dissipation, high self-centering and negligible damage. Both HSR member types demonstrated the ability to control of the applied seismic loading.

5. ACKNOWLEDGMENTS

The authors would like to acknowledge the Federal Highway Administration of the U.S. Department of Transportation for providing funding for this research through the Multidisciplinary Center for Earthquake Engineering Research (MCEER) of the University at Buffalo – The State University of New York. The Bodossaki Foundation and the Alexander S. Onassis Public Benefit Foundation are also acknowledged for providing partial financial support to the first author. The help of Ms. Myrto Anagnostopoulou, structural and test engineer at SEESL of the University at Buffalo in the preliminary design of the test specimen is also acknowledged.

REFERENCES

- AASHTO LRFD Bridge Design Specifications (2007). "AASHTO LRFD Bridge Design Specifications, 4th Edition." American Association of State Highway and Transportation Officials (AASHTO), 444 North Capitol Street, NW, Suite 249, Washington, DC 20001.
- ASCE/SEI 7-05 (2006). "Minimum design loads for buildings and others Structures." American Society of Civil Engineers (ASCE), Reston, VA.
- ATC/MCEER Joint Venture (2003). "MCEER/ATC-49: Recommended LRFD Guidelines for the Seismic Design of Highway Bridges." *Part I: Specifications and Part II: Commentary and Appendices*, MCEER-03-SP03, Multidisciplinary Center for Earthquake Engineering Research (MCEER) / Applied Technology Council (ATC).
- Chopra, A. K. (2001). *Dynamics of structures: theory and applications to earthquake engineering*, 2nd Edition, Prentice Hall.
- FEMA P695 (2009). "Quantification of Building Seismic Performance Factors." Federal Emergency Management Agency, Washington, D.C.
- Megally, S. H., Garg, M., Seible, F., Dowell, R. K. (2002). "Seismic Performance of Precast Segmental Bridge Superstructures." Report No. SSRP-2001/24, Department of Structural Engineering, University of California, San Diego, La Jolla, California 92093-0085.
- PCI Bridge Design Manual (2003). "Precast/Prestressed Concrete Bridge Design Manual, 2nd Edition." Precast/Prestressed Concrete Institute (PCI), 209 W. Jackson Blvd. #500, Chicago, IL 60606 - 312.786.0300.
- Sideris, P. (2012). "Seismic Analysis and Design of Precast Concrete Segmental Bridges." Ph.D. Dissertation, State University of New York at Buffalo, Buffalo, NY, U.S.A.
- Sideris, P., Aref, A. J., Filiatrault, A. (2012). "Seismic Testing of a Hybrid Sliding-Rocking Post-Tensioned Segmental System." *Journal of Structural Engineering (Under Review)*.